New Thermoplastic Elastomers based on Ethylene-Butadiene-Rubber (EBR) by Switching from Anionic to Coordinative Chain Transfer Polymerization

Samy Alioui, Marvin Langlais, Robert Ngo, Karima Habhab, Séverin Dronet, François Jean-Baptiste-Dit-Dominique, David Albertini, Franck D'Agosto, Christophe Boisson, Damien Montarnal

New Thermoplastic Elastomers based on Ethylene-Butadiene-Rubber (EBR) by Switching from Anionic to Coordinative Chain Transfer Polymerization

Samy Alioui,[a] Marvin Langlais,[a] Robert Ngo,[b] Karima Habhab,[b] Séverin Dronet,[b] François Jean-Baptiste-dit-Dominique,[b] David Albertini,[c] Franck D'Agosto,*[a] Christophe Boisson*[a] and Damien Montarnal*[a]

[a] S. Alioui, Dr. M. Langlais, Dr. F. D'Agosto, Dr. C. Boisson, Dr. D. Montarnal
Université Claude Bernard Lyon 1, CPE Lyon, CNRS UMR 5128, Laboratoire CP2M, Equipe PCM, 69616 Villeurbanne, CEDEX, France
E-mail: damien.montarnal@univ-lyon1.fr, christophe.boisson@univ-lyon1.fr, franck.dagosto@univ-lyon1.fr
[b] R. Ngo, K. Habhab, Dr. S. Dronet, Dr. F. Jean-Baptiste-dit-Dominique
Manufacture Michelin, 23 place Carmes Déchaux, F-63000 Clermont-Ferrand, France
[c] D. Albertini
Université Claude Bernard Lyon 1, CNRS, INSA Lyon, Ecole Centrale de Lyon, CPE Lyon, INL, UMR5270, 69622 Villeurbanne, France

Abstract: Olefin triblock copolymers based on glassy polystyrene (PS), ethylene butadiene rubber (EBR) and highly crystalline polyethylene (PE) segments were prepared for the first time using a switch strategy from anionic polymerization to coordinative chain transfer (co)polymerization (CCT(co)P). PS chains obtained by anionic polymerization were transmetalated with mesitylmagnesium bromide (BrMgMes) to act as macromolecular chain transfer agents (macro-CTA, PS-MgMes) in the CCTcoP of ethylene and butadiene using $\{Me_2Si(C_{13}H_8)_2Nd(BH_4)_2Li(THF)\}_2$ complex (**1**). Further chain extension by CCTP using pure ethylene in the monomer feed afforded well-defined PS-*b*-EBR-*b*-PE triblock copolymers. The structural, rheological and mechanical properties of these materials demonstrate excellent balance between properties and easy processability at moderate temperatures (> 150 °C). We demonstrate that such triblock copolymers behave effectively as low-viscosity PS-*b*-EBR diblock copolymers above the melting point of PE domains and high performance thermoplastic elastomers (TPEs) upon crystallization of PE segments.

Introduction

Thermoplastic elastomers (TPEs) are an important class of elastomer materials that combines the processing advantages and recycling potential of thermoplastic with the flexibility, low modulus and soft touch of thermoset rubbers. They are thus fulfilling the requirements for a sustainable circular economy for the next generation of plastics.[1] Many TPEs are copolymers that derive their elastomeric properties from an architecture combining hard (semi-crystalline or glassy) and soft blocks that leads to phase-separated and connected domains at service temperatures. High elastic recoveries akin to permanently crosslinked elastomers can be achieved in structures featuring soft segments, separated by at least two hard segments self-assembling into dispersed domains and acting as physical crosslinks. Additional requirements such as low moduli and high extensibility also are that the soft segments are well-entangled and constitute a continuous phase.[2] This type of TPEs generally involves architectures such as Hard-Soft-Hard linear triblock, $(Hard\text{-}Soft)_n$ linear multiblock or linear branched copolymers. Styrenic triblock copolymers are commercial examples featuring polystyrene (PS) outer segments and polyisoprene (PIP) (PS-*b*-PIP-*b*-PS) or (potentially hydrogenated) polybutadiene (PB) (PS-*b*-PB-*b*-PS, PS-*b*-P(ethylene-*co*-butylene)-*b*-PS) as the rubbery middle segment.[3] These TPEs can reach tensile strengths of 30 MPa. Besides the number-average molar mass (M_n), one of the key parameters controlling the melt viscosity and processability of these copolymers is their mechanism of phase separation. Copolymers featuring highly immiscible segments remain nanophase-separated above the glass transition temperature (T_g) or the melting temperature (T_m) of the hard segments. These TPEs, referred thereafter as *strongly separated TPEs*, display thus (very) high melt viscosities. Bates and coworkers have shown for example that linear $(PS\text{-}b\text{-}PIP)_n$ multiblock copolymer display zero-shear viscosities varying with the number of blocks as $n^{7.5}$.[4]

Alternatively, to strongly separated TPEs, other TPEs comprise segments partially or fully miscible at high temperatures that undergo crystallization-induced phase separation at low temperatures. In comparison to strongly separated TPEs, such copolymers, that we refer to as *crystallization-induced TPEs*, display reduced tensile strength, with a maximum well below 20 MPa, and also demonstrate lower elastic recoveries because of easy chain pullout or plastic deformation in crystalline domains. Yet, these TPEs are much easier to process thanks to their low melt viscosity.[5] This category is well illustrated by polyolefin elastomers, typically consisting in polymer chains with randomly distributed ethylene and α-olefin units.[6] Polyolefin elastomers can generally be obtained by random, tandem or by chain walking polymerization.[7–9] The insertion of α-olefin into PE chains forms short chain branches, which partially disrupt the crystal structure, resulting in the formation of a rubber phase and a ductile crystalline phase. Commercial grades such as ENGAGE™ and Exxpol™ can achieve high crystallinity but their service temperature is rather limited by the low T_m of PE segments (< 104 °C).

Finding new compromises between processability and performance (service temperature, mechanical properties) of polyolefin thermoplastic elastomers is thus an active ongoing field of research. The control over the copolymerization of olefins into well-defined macromolecular architectures has made decisive progress with the establishment of living coordination-insertion polymerization that allows the successive growth of polymer chains into block structures.[10,11] However, only one polymer chain is produced per metal active center, which considerably increases the overall cost and the amount of metallic residues, and therefore reduces the possibility of producing these polymers on a large scale. In 2015, Coates and coworkers reported graft copolymers by copolymerizing allyl-terminated syndiotactic or isotactic polypropylene macromoners

with olefins. This modular approach has permitted the incorporation of semi-crystalline polypropylene side chains into amorphous backbones containing ethylene and α-olefin units.[12] TPEs with excellent properties are obtained: melting temperatures up to 140 °C, tensile strengths above 10 MPa, extensibility above 1000 % with elastic recoveries above 85 %. Nevertheless, this two-stage polymerization requires the isolation of polypropylene macromonomers. Advanced techniques such as coordinative chain transfer polymerization (CCTP) allows the generation of a large number of polymeric chains per metallic active center while allowing a very good control over their growth, which is critical for the economical relevance of the commodity polymers to which this technique gives access. This controlled coordination-insertion polymerization technique takes advantage of a degenerative chain transfer between the metallic active center serving as a catalyst and an organometallic chain transfer agent (CTA) such as MgR_2, AlR_3 or ZnR_2.[13–16] Diblock and multiblock copolymers have been synthesized via CCTP by controlling sequentially the monomer feed. Even more remarkably, the combination of two catalysts with a common CTA (called in this case chain shuttling agent (CSA)), e.g. such as $ZnEt_2$, can polymerize a common feed of monomers (e.g. ethylene and 1-octene) to alternatively grow semi-crystalline polyethylene (PE) and amorphous poly(ethylene-*co*-1-octene) blocks on a single chain.[17] Such multiblock copolymers are now commercialized by Dow Chemical under the tradename INFUSE™. Lee and coworkers have successfully prepared by CCTP PE-*b*-poly(ethylene-*co*-propylene)-*b*-PE (PE-*b*-PEP-*b*-PE) triblock copolymers by successive polymerization of ethylene, a mixture of ethylene (E) and propylene (P), and finally a coupling reaction to form the triblock.[18] The same group developed a zinc-based divalent chain transfer agent.[19] PS-*b*-PEP-*b*-PS triblock and PS-*b*-PEP diblock copolymers were obtained by coordinative chain transfer copolymerization (CCTcoP) of E with P using a pyridyl-amido hafnium catalyst followed by anionic polymerization of styrene. They also described an original zinc-based CTA bearing an α-methylstyrene moiety that was retained during the CCTcoP of E and P performed in combination with *ansa*-metallocene zirconium catalyst. The obtained telechelic polyolefins (POs) were used to initiate the anionic polymerization of styrene (S) using Me_3SiCH_2Li·(pentamethyldiethylenetriamine) to lead to triblock PS-*b*-PO-*b*-PS.[20]

CCTcoP of ethylene and butadiene (B) can be carried out with the complex $\{Me_2Si(C_{13}H_8)_2Nd(BH_4)_2Li(THF)\}_2$ (**1**) in combination with dialkylmagnesium or divalent Grignard CTAs.[21–23] This strategy produces block copolymers with ethylene units, *trans*-1,4 and vinyl butadiene units and cyclohexyl motifs on one segment, also called ethylene butadiene rubber (EBR) segment, and highly crystalline PE segments. Triblock PE-*b*-EBR-*b*-PE and multiblock EBR-(PE-*b*-EBR)$_2$ copolymers displaying crystallization-induced phase separation showed good performance as TPEs in terms of extensibility (> 1000 %) and elastic recovery (> 85 %), but their tensile strength (< 6 MPa) remains limited by the ductile domains formed by too short PE segments.[24]

Strongly separated TPEs and crystallization-induced TPEs have their own merits, such as high tensile strength and low viscosity, respectively. It is thus tempting to combine both behaviors using asymmetric triblock copolymers ABC where A strongly segregates from B and C, B is a rubbery segment, and C is a highly crystalline segment. Abetz and coworkers have compared in this way PS-*b*-PEP-*b*-PS (SEPS) and PS-*b*-PEP-*b*-PE (SEPE) synthesized by sequential anionic polymerization of styrene, isoprene and butadiene and subsequent hydrogenation.[25,26] While such syntheses gave relatively poorly crystalline PE segments (T_m < 90 °C), SEPE could reach tensile strength up to 30 MPa and benefits in comparison to SEPS could even be detected in the elastic recovery at low strains.

Attaining such ABC architectures with POs, and in particular with EBR is indeed compatible with CCT(co)P, particularly when relying on the unprecedented concept of switch from anionic polymerization to CCTP that we recently described.[27] In the present work, the preparation of a large range of PS-*b*-EBR-*b*-PE triblock copolymers is reported. The strategy employed is based on the *in situ* preparation of a macromolecular chain transfer agent obtained by anionic polymerization of styrene, followed by sequential CCTcoP of E and B, and CCTP of E. Structural, mechanical and rheological characterizations are performed on the resulting copolymers to highlight the potential of these new TPEs.

Results and Discussion

Synthesis of diblock copolymers via successive anionic polymerization and CCTcoP

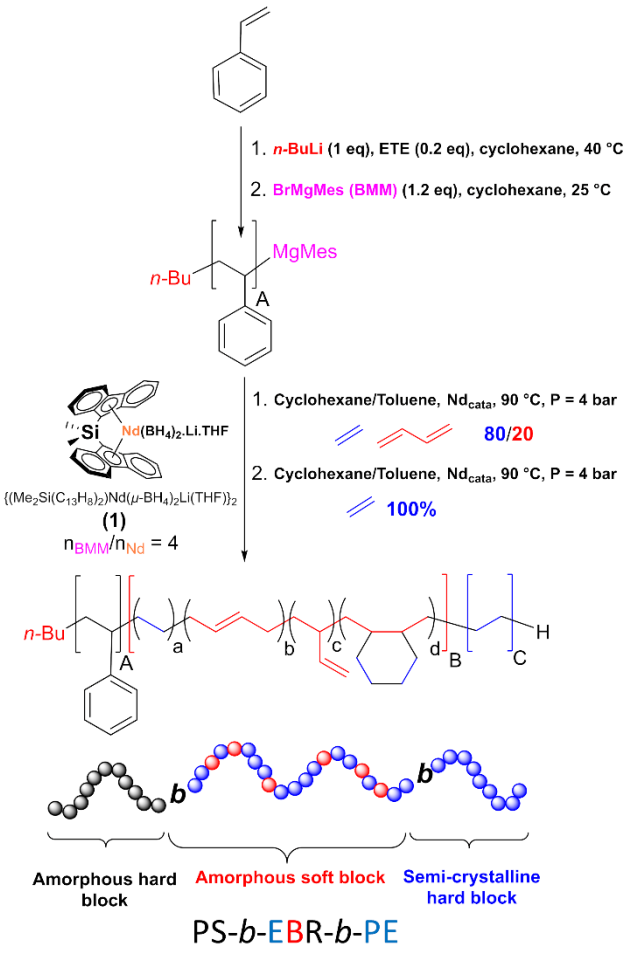

Scheme 1 Synthesis of triblock copolymers using **1**/PS-MgMes catalyst

We have previously reported the synthesis PS-*b*-EBR by the switch from anionic polymerization to CCTcoP in toluene. In the present work, the protocol was improved to limit the formation of PS dead chains observed in toluene and circumvent the solubility issue of PS-MgMes encountered in methylcyclohexane (Fig. S1 and S2). The anionic polymerization step was carried out here in cyclohexane at 40 °C using *n*-BuLi as initiator and ethyl tetrahydrofurfuryl ether (ETE) (n_{ETE}/n_{Li} = 0.2) as polar agent. The amount of *n*-BuLi was varied according to desired M_n of the targeted PS. After 20 minutes, an excess of mesitylmagnesium bromide (MesMgBr) (n_{Mg}/n_{Li} = 1.2) was added to the reaction medium to turn PS-Li chains into PS-MgMes (Scheme 1 and Fig. S3). SEC analyses of PS aliquots isolated after the anionic polymerization step showed good agreement of the obtained M_n with the targeted M_n, and low dispersities characteristic of living polymerization (Fig. S4, Table S1).

To form the second EBR block by CCTcoP, the PS-MgMes solution was contacted with the catalyst solution (obtained by reacting **1** with an excess of MesMgBr, ($n_{MesMgBr}$ / n_{Nd} = 4) at 90 °C) and then pressurized with 4 bar of a mixture of E and B (80/20 mol/mol). The reaction was then stopped when the pressure drop indicated a monomer consumption of 15 g. Several diblock copolymers were targeted (Table 1). Diblock copolymers of increasing M_n (Table 1, runs 1-3) were synthesized keeping the same fraction of PS (~33 wt%). For the sake of clarity, a polymer segment P with a M_n of X kg mol^{-1} will be denoted P_{Xk}. SEC analyses of PS aliquots and of the corresponding diblock copolymers showed successful chain extensions (Fig. S5). The M_n obtained are in agreement with the targeted M_n. The low dispersity (*Đ*) values measured for these copolymers are characteristic of CCTcoP polymerization. The SEC chromatograms also show the presence of shoulders corresponding to PS fractions that have not undergone chain extension when PS with M_n higher than 10 kg mol^{-1} are used. This was confirmed after a block copolymer purification step, in which the unreacted PS fraction was eliminated (Fig. S5, S6). For the copolymers with a M_n of PS of 10 kg mol^{-1}, PS_{10k}, no shoulder was observed. The absence of a shoulder could be due to better accessibility of PS chains of low M_n for chain transfer during the CCTcoP step.

A series of diblock copolymers based on a PS with a targeted PS_{20k} with an increasing fraction of EBR were also prepared (Table 1, Runs 4-6). After chain extension of PS, a broadening of the molar mass distribution is observed for the highest targeted EBR M_n (Table 1, Fig. S5 and S6, runs 5 and 6). This broadening could be due to an increase in the viscosity of the medium, which might slow down the exchange rate between the active and dormant species.

Finally, the six diblock copolymers displayed very similar microstructures (Table S2) and the fraction of PS determined by ^{1}H NMR is close to the targeted one (Table 1).

Table 1. Yield, molar mass characteristics and thermal properties of PS-*b*-EBR diblock copolymers before purification.

Run	Block copolymer	[PS-MgMes] mmol L^{-1}	Yield g	M_n $^{theo\ [a]}$ kg mol^{-1}	M_n $^{SEC\ [a]}$ kg mol^{-1} (*Đ*) $^{[a]}$	T_g $^{EBR\ [c]}$ °C	PS fraction $^{[d]}$ wt%	Targeted PS fraction wt%
1	PS_{10k}-*b*-EBR_{20k}	3.750	22.6	30 100	34.7 (1.25)	-29	31.8	33
2	PS_{20k}-*b*-EBR_{40k}	1.875	22.0	59 000	56.6 (1.37)	-30	30.3	33
3	PS_{30k}-*b*-EBR_{60k}	1.250	23.9	95 600	90.5 (1.60)	-30	31.4	33
4	PS_{20k}-*b*-EBR_{30k}	2.500	24.4	48 800	51.4 (1.36)	-29	39.3	40
5	PS_{20k}-*b*-EBR_{60k}	1.250	18.7	74 800	59.2 (2.00)	-32	25.2	25
6	PS_{20k}-*b*-EBR_{80k}	0.937	19.2	102 500	80.4 (2.00)	-30	18.7	20

Xk stands for X* kg mol^{-1} and designates the targeted M_n of the considered chain. Conditions for S anionic polymerization: *n*-BuLi = 1 equivalent, ETE = 0.2 equivalent, $m_{cyclohexane}/m_{styrene}$ = 7, T = 40°C, reaction time = 20 min. Conditions CCT(co)P: toluene + cyclohexane = 200 mL, MesMgBr = 200 µmol (n_{Mg}/n_{Nd} =4), P = 4 bar (E/B = 80/20 mol/mol), T = 90 °C, [Nd] = 250 µM. [a] M_n theo = yield/($n_{PS\text{-}MgMes}$). [b] Determined by SEC in THF at 35 °C using a conventional calibration with PS standards. [c] Determined by DSC. [d] Determined by ^{1}H NMR in $CDCl_3$ at 25 °C..

Synthesis of triblock copolymers via successive anionic polymerization, CCTcoP and (CCTP)

A first triblock copolymer PS_{3k}-*b*-EBR_{30k}-*b*-PE_{6k} was targeted (Table 2, run 7). The intermediate diblock copolymer PS_{3k}-*b*-EBR_{30k} was obtained following the procedure described in the first section. Indeed, **1** and PS-MgMes macro-CTA were used to copolymerize E and B. A change in monomer feed from E/B (80/20 mol/mol) to E was performed for the formation of the third PE block (Scheme 1, Fig. S7). The ethylene consumption and thus the M_n of the PE block was determined by following the pressure drop in the feed tank. The feed was stopped when the desired monomer consumption was reached (1.5 g).

In order to develop useful TPEs, it was essential to increase the M_n of triblock copolymers to achieve a high entanglement of the EBR segment. A triblock copolymer with a M_n of EBR block of 60 kg mol^{-1} was further targeted. In this case, to prevent i*n situ* precipitation of the growing chains when the PE block forms, it is important to control the concentration of chains in the polymerization medium. The macro-CTA concentration was then reduced ; as expected, an increase in the M_n of the EBR block

was observed (Table 2, runs 7-8). SEC traces of these two copolymers based on an initial PS_{3k} segment (Fig. S9, runs 7-8) are unimodal highlighting the formation of the desired triblock copolymers. On the other hand, dispersities increased significantly as the M_n of the triblock copolymer increase. This is certainly due again to the viscosity of the medium, which makes exchanges between the dormant polymer-[MgMes] species and the propagating polymer-[Nd] species slower. The M_n of the final PE segment is constrained by the polymerization conditions: chains longer than 6 kg mol^{-1} may lead to precipitation and loss of control at 90°C, while higher polymerization temperatures favor β-H eliminations.[28,29]

The relevance of this synthesis method allowed us to prepare a series of $PS_{3\text{-}20k}$-*b*-EBR_{60k}-*b*-PE_{6k} triblock copolymers. The aim was to fix the M_n of the EBR and PE blocks at 60 kg mol^{-1} and 6 kg mol^{-1}, respectively, and to vary the M_n of the PS block from 3 to 20 kg mol^{-1} (varying the content of PS block from 7.7 to 23.3 wt%). SEC-THF analysis of the PS aliquots corresponding to each triblock copolymer showed the M_n obtained are close to those targeted and narrowly distributed, as expected for anionic polymerization (Fig. S8, Table S3). Triblock copolymers were analysed by high temperatures SEC (HT-SEC) using trichlorobenzene as eluent and operating at 150 °C. The evolution of the M_n of the triblock copolymers is an indication of the extension of the PS chains (Table 2, runs 7-12). In run 9-12 (Fig. S9), the SEC trace shows the presence of a negative signal assigned to the presence of unreacted PS chains. This is not the case for runs 7-8, for which a PS_{3k} is employed. This could be due to a less efficient transmetalation of PS chains to neodymium when increasing the M_n of the PS block. The ratio between Vinyl-units, *trans*-1,4-units and 1,2-cyclohexyl motifs is very similar for the triblock copolymers (Table S4, Fig. S11) demonstrating that the EBR blocks have the same microstructure. As expected, there is also a good agreement between targeted and experimental wt% of PS in copolymers (Table 2, run 7-12).

Table 2. Yield, number-average molar mass features and thermal properties of PS-*b*-EBR-*b*-PE triblock copolymers.

Run	Block copolymer	[PS-MgMes] mmol L^{-1}	Yield g	M_n $^{theo\ [a]}$ kg mol^{-1}	M_n $^{SEC\ [b]}$ kg mol^{-1} ($Đ$) [b]	T_g $^{EBR\ [c]}$ °C	Tm $^{PE\ [c]}$ °C	Tc $^{PE\ block\ [c]}$ °C ($\Delta Hm/Xc^{PE}$) [d] J g^{-1} / %	PS fraction[e] (targeted) wt%
7	PS_{3k}-*b*-EBR_{30k}-*b*-PE_{6k}	2.50	17.1	34.2	61.0 (1.5)	-31	122	102 (31.4/ 70)	6.4 (7.7)
8	PS_{3k}-*b*-EBR_{60k}-*b*-PE_{6k}	1.25	18.8	75.2	93.2 (2.2)	-32	120	91 (17.1/ 67)	3.7 (4.5)
9	PS_{6k}-*b*-EBR_{60k}-*b*-PE_{6k}	1.25	18.0	72.0	113.6 (2.1)	-28	115	76 (11.7/ 48)	7.0 (8.3)
10	PS_{10k}-*b*-EBR_{60k}-*b*-PE_{6k}	1.25	17.7	70.6	118.7 (1.8)	-30	115	78 (10.6/ 46)	12.6 (13.2)
11	PS_{15k}-*b*-EBR_{60k}-*b*-PE_{6k}	1.25	20.7	82.8	149.1 (2.1)	-31	121	90 (7.9/ 36)	20.3 (18.5)
12	PS_{20k}-*b*-EBR_{60k}-*b*-PE_{6k}	1.25	21.5	86.0	154.2 (1.7)	-29	120	88 (12.2/ 60)	22.9 (23.3)

Xk stands for X* kg mol^{-1} and designates the targeted M_n of the considered chain. Conditions for S anionic polymerization: *n*-BuLi = 1 equivalent, ETE = 0.2 equivalent, $m_{cyclohexane}/m_{styrene}$ = 7, T = 40 °C, reaction time = 10 min. Conditions CCT(co)P: toluene + cyclohexane = 200 mL, MesMgBr = 200 µmol (n_{Mg}/n_{Nd} =4), P = 4 bar (E/B = 80/20 mol/mol for EBR block and E = 100 for PE block), T = 90 °C, [Nd] = 250 µM. [a] M_n theo = yield/($n_{PS\text{-}MgMes}$). [b] Determined by SEC in THF at 35°C using a conventional calibration with PS standards. [c] Determined by DSC. [d] Melting enthalpy of PE determined by DSC, and crystallinity normalized to the PE content. [e] Determined by ^{1}H NMR in TCE/C_6D_6 (2/1 v/v) at 90 °C.

Thermomechanical and rheological properties

DSC analysis (Table 1 and S1, Fig. S12) of the diblock copolymers shows a T_g for the PS block at about 100 °C and that of EBR segments at about -30 °C, consistent with a strong phase segregation. A large and weak melting endotherm related to EBR segments at about 20 °C is also detected. For triblock copolymers (Table 2 and S3, Fig. 1.a, Fig. S13), the T_g of the EBR block is observed at about -30°C, the T_m of the PE block is in the range of 115-122 °C and the crystallization temperature varies between 76 and 102 °C. The T_g of the PS block cannot be determined on the final triblocks as it overlaps with the melting of PE. Instead, we chose to indicate the T_g of the initial PS block determined from aliquots withdrawn after the anionic polymerization step (Table S3). The shortest segments (PS_{3k}) lead to T_gs about 60 °C while $PS_{6\text{-}20k}$ segments reach T_gs of 90-95 °C (Table S3). PE crystallinities (see Table 2) are relatively high, up to 70 % for triblocks featuring short PS blocks (PS_{3k}), and continuously decrease when the M_n of PS blocks increase. An exception was found for run 12, which displayed a particularly high crystallinity of 60 %. We found a significant presence of PE homopolymer in this polymer (Fig. S10), probably resulting from a side reaction. Indeed, as mentioned above, when high M_n copolymers are synthesized, the viscosity of the medium increases, the exchange of active and dormant species becomes slower and this favors β-H elimination reactions.

Thermomechanical characterization between -80 °C and 160 °C was obtained from DMA in tensile mode or in shear mode (Fig. 1b, Fig. S14). For diblock copolymers, the α-transitions for EBR and PS domains are clearly separated (Fig. S14). The run series 1-3 features PS-*b*-EBR diblock copolymers with a common target of 33 wt% PS and increasing M_n. Over the series, a strong

decrease in the dissipation can be seen (Fig. S14b), associated to a more stable storage moduli over the service temperature range 25-80 °C (Fig. S14a). The run series 4-6 features diblock copolymers with the same PS_{20k} block and increasing M_n EBR blocks. The dissipative properties are then constant in the 25-80 °C range (Fig. S14d), which directly links these properties to the PS block and indicate that the entanglement molar mass of PS should be targeted. The storage moduli strongly increase with the fraction of PS as expected from phase-separated diblock copolymers that should transition from spherical or cylindric morphologies to lamellae. All diblock copolymers demonstrate significant stability of moduli above T_g of PS and up to 160 °C. This indicates an absence of flow, at least at very small deformations, that we attribute to a nanostructuration between PS and EBR domains. Key indicators have been gathered in Tables S5 and S6, including the ratio $E'^{25\,°C}/E'^{80\,°C}$ that quantifies the stability of the modulus in the service range and the loss

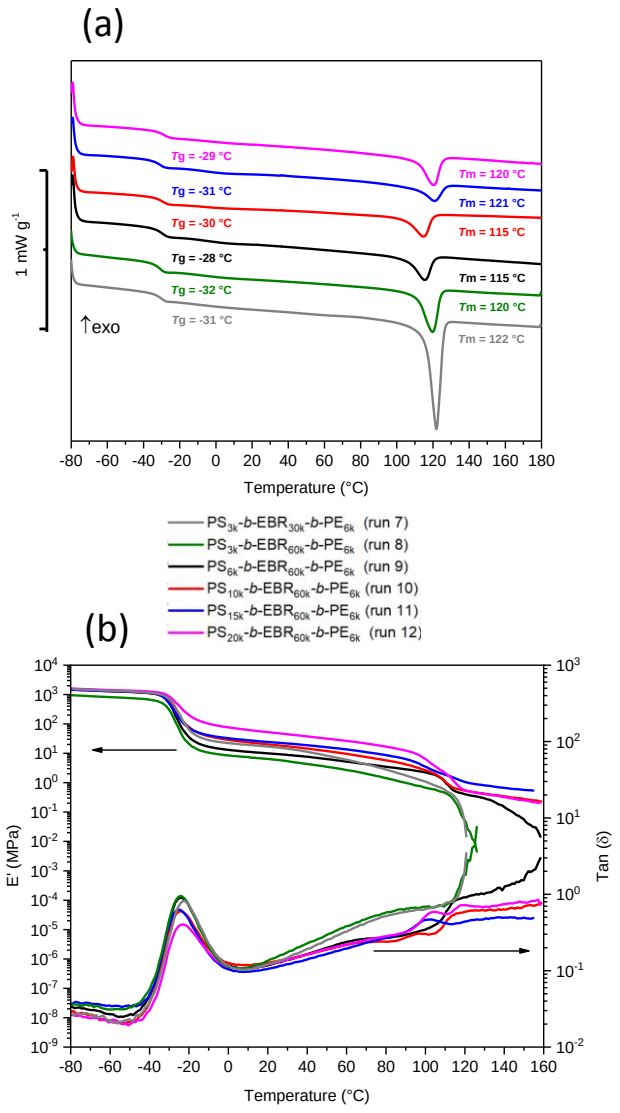

factors at 25 °C and 80 °C that quantify the dissipation. Good compromises (i.e. lower values for this ratio) for elastomers (i.e. $E'^{80\,°C}$ < 10 MPa) are found in cases where the EBR segment is sufficient large (>60 kg mol^{-1}) and the rigid PS segment acts as a minor block. The PS_{20k}-*b*-EBR_{60k} copolymer (run 5) being a relevant example, we will therefore focus on EBR_{60k} segments in the study of triblock copolymers. Run 7 (PS_{3k}-*b*-EBR_{30k}-*b*-PE_{6k}) enables comparison with low M_n while the run series 8-12 (PS_{ak}-*b*-EBR_{60k}-*b*-PE_{6k}) targets increasing molar masses of PS block and constant molar masses for EBR and PE blocks.

Figure 1 - (a) DSC thermograms of the PS-b-EBR-b-PE triblock copolymers obtained with **1**/PS-MgMes catalyst (-80 to 180 °C, 10 °C min^{-1}). (b) DMA analysis of triblock copolymers in tensile mode (1 Hz, 3 °C min^{-1}, -100 to 160 °C).

DMA (Fig. 1b, Table S7) indicates an immediate drop of moduli above T_g of PS for the shortest blocks (PS_{3k}, runs 7 and 8), and in a lesser extent for run 9 with a PS_{6k} block. This would indicate that nanostructuration in the melt is either absent or very weak in such cases. In contrast, all samples with PS blocks with molar masses higher than 10 kg mol^{-1} demonstrate an absence of flow as seen in diblocks. The moduli at 25 °C for runs 8-12 increased from 5.9 MPa to 47.8 MPa as the PS fraction varied from 4.5 to 23.3 wt% and the T_g of EBR segment remains around -30 °C in all cases. The triblocks displayed in general a better stability of the rubbery regime at high temperatures than the diblocks. The loss factor (tan(δ) value) at 80 °C is particularly indicative in this regard and decreases from 0.37 (run 5, PS_{20k}-*b*-EBR_{60k}) to 0.24-0.28 for comparable samples (runs 10-12 $PS_{10/15/20k}$-*b*-EBR_{60k}-*b*-PE_{6k}). We also note that the tan(δ) values of $PS_{10/15/20k}$-*b*-EBR_{60k}-*b*-PE_{6k} triblock copolymers are significantly lower than the value previously found for PE_{6k}-*b*-EBR_{60k}-*b*-PE_{6k}.

Melt viscosity at 150 °C and 200 °C was analyzed by flow and dynamic rheology (Fig. S15-S19). As previously perceived, only the copolymers with the shortest PS segments (PS_{3k}, runs 7 and 8) display a fully Newtonian behavior (Fig. S16) and a terminal regime characteristic of unstructured liquids (Fig. S19 - $G'\sim\omega^2$, $G''\sim\omega^1$). All other copolymers, diblocks or triblocks display significant elasticity, with slopes of $G'(\omega) < 0.5$ (Fig. S19), and correspondingly reach very high zero-shear viscosities, with measured values at 0.01 s^{-1} reaching above 10^6 Pa s. The evolution of these viscosities with the M_n of the samples measured by SEC is reported in Fig. S17. The strong dependency, well beyond $\eta_0 \sim M_n^{3.4}$ clearly indicates the presence of nanostructured liquids. We note that the PS_{20k}-*b*-EBR_{60k}-*b*-PE_{6k} copolymer (Fig. S16a, run 12) showed an unexpectedly low viscosity that may be due to the presence of PE homopolymer in the final material (Fig. S10). Comparisons between diblocks and triblocks with similar PS fraction: run 6 (PS_{20k}-*b*-EBR_{80k}) vs run 11 (PS_{15k}-*b*-EBR_{60k}-*b*-PE_{6k}) give similar viscosities, indicating that the presence of the third PE block does not impact the viscosities, and suggesting that the PE segment is fully miscible with the EBR in the melt. While the viscosities are relatively high, a significant shear-thinning behavior is found for these copolymers (Fig. S15-S16, up to 1 decade drop of viscosity as the shear rate is increased from 0.01 to 1 s^{-1}) that prefigures possible processability. In practice, the compression molding of all samples at 180 °C for a few minutes gave defect-free plates.

Structural analysis

Structural analysis of the samples was provided by temperature-dependent SAXS using synchrotron facilities (Swing@Soleil). Compression molded samples were initially heated to 165 °C, i.e. well above T_m of the PE segments, then stepwise cooled and analyzed (Fig. S20-S22). Each step was thermally equilibrated for 10 min.

First, the analysis of the amorphous PS-*b*-EBR diblocks (Fig. S20-S21) showed clear Bragg scattering peaks and

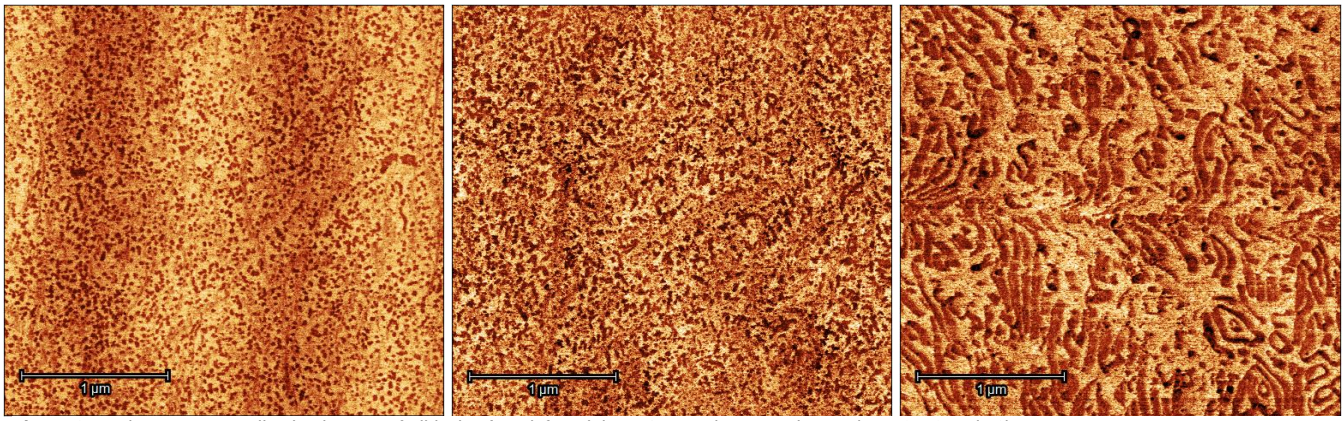

Figure 2. Peak-Force AFM adhesion images of triblocks; from left to right: $PS_{6/10/20k}$-*b*-EBR_{60k}-*b*-PE_{6k} (runs 9, 10 and 12).

corresponding harmonics indicating microphase separation in all cases. The inter-domain spacing increases with the M_n of the copolymers as d ~ $M^{0.7}$(Fig. S23), i.e. with an exponent close to the theory for strong segregation (2/3). While diblocks with low M_n (< 60 kg mol^{-1}) display relatively narrow scattering peaks and a high number of harmonics, consistent with narrow interfaces and long-range ordering, samples with higher M_n were significantly less ordered. We attribute these changes to the absence of specific attempts at improving the self-assembly (e.g. solvent or thermal annealing); achieving long-range ordering with high viscosity materials is indeed a very slow process. For this reason also, it is difficult to determine the exact nature of the structuration. A lamellar organization is relatively clear for runs 1 (PS_{10k}-*b*-EBR_{20k}) and 4 (PS_{20k}-*b*-EBR_{30k}) with n.q_0 harmonics while additional harmonics might be present to indicate cylinders in run 2 (PS_{20k}-*b*-EBR_{40k}). Concerning the triblocks (Fig. S22), the structuration appears also strongly segregated in the melt at 165 °C, although runs 8 (PS_{6k}-*b*-EBR_{60k}-*b*-PE_{6k}) and 9 (PS_{10k}-*b*-EBR_{60k}-*b*-PE_{6k}) demonstrate very low d-spacing values that could be related to a different morphology (spheres rather than cylinders or lamellae) caused by the very low fraction of PS in these triblocks. Interestingly, the diffractograms only show little changes upon crystallization of PE (Fig. S22 - data at 87 °C): the position of the main scattering peaks and their harmonics is barely impacted; the changes in intensity might be related to variation in the scattering length density of the EBR-PE domains. This demonstrates that the crystallization is confined within the EBR-PE domains by the rigid PS domains, consistently with the hard confinement expected as the T_g of PS domains is higher than the crystallization temperature of PE segments.

Peak-Force AFM measurements were further carried out on surfaced samples of triblocks (run 9-10 and 12) to provide more specific analysis of the bulk morphologies. Adhesion mappings are shown in Fig. 2, they display a high contrast between PS domains (dark – low adhesion) and EBR/PE domains (light – high adhesion). PS domains are rather spheroids for PS_{6k}-*b*-EBR_{60k}-*b*-PE_{6k} (run 9), close to the bicontinuity for PS_{10k}-*b*-EBR_{60k}-*b*-PE_{6k} (run 10) and cylinders for PS_{20k}-*b*-EBR_{60k}-b-PE_{6k} (run 12).

The stiffness mapping (Fig. S24, light - high stiffness) gives complementary information and enables to differentiate the crystalline PE domains, under the form of platelets or fibers about 30 nm thick and up to 1 µm large. These structures can also be seen on the adhesion mapping (Fig. 2, runs 9 and 10) as thin stripes growing across the PS domains. This further confirms that crystallization of PE is hard-confined by the PS domains.

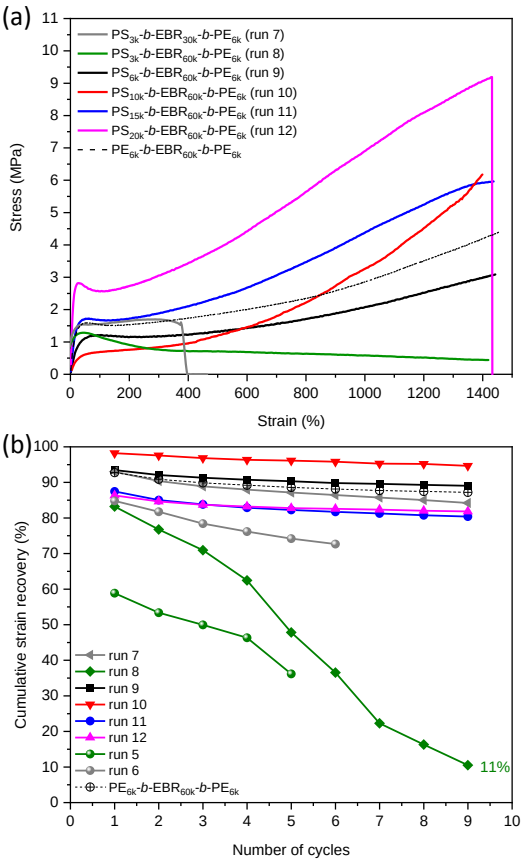

Figure 3 - (a) Tensile testing of triblock copolymers (RT, 500 mm min^{-1}). 1450 % elongation corresponds to the maximal course and indicates that the samples did not break during test. (b) Elastic recovery after cyclic extension of the samples up to 300% elongation (RT, 500 mm min^{-1}).

Tensile properties

Tensile test were performed to determine some of the basic mechanical properties of our block copolymers, such as strain at break (ε_b), tensile strength at break (σ_b), and elastic recovery after 10 successive deformations at 300 % strain (Fig. 3, Fig. S25). Diblock copolymers with high fractions of PS (≥ 33 wt%,

runs 1-4) exhibit a fragile behavior, with high moduli, a yield point at about 50 % elongation typical of semi-crystalline materials, followed by rupture. Softer diblocks (PS fraction ≤ 25 wt%, runs 5, 6) exhibit a lower yield stress and viscoplastic profiles with large deformations but low decaying stresses (Fig. S25). The M_n appears critical at such high strain regimes, and the cumulative strain recovery after multiple extension cycles (Fig. 3b, Fig. S26) shows much better performances for the highly entangled PS_{20k}-*b*-EBR_{80K} (run 6) in comparison to PS_{20k}-*b*-EBR_{60k} (run 5).

In regards to triblock copolymers, the PS_{3k}-*b*-EBR_{30k}-*b*-PE_{6k} and PS_{3k}-*b*-EBR_{60k}-*b*-PE_{6k} also show plastic deformation after the yield point thus confirming the absence of phase separation anchoring the EBR matrix to PS domains. All other triblocks showed a strain hardening starting from 500 % strain (Fig. 3a), confirming this time that the rubbery EBR segments are efficiently anchored at both extremities. Triblock copolymers with a 6-15 kg mol^{-1} PS block showed an elastomeric behavior with an absence of a yield point, an elongation of more than 1450 % with significant strain hardening and a high elastic recovery above 80 % after 9 elongation cycles demonstrating significant dimensional stability under load (Fig. 3b and S27).
This is consistent with their morphologies, revealed above with AFM, which consist in dispersed PS domains and PE platelets forming within the EBR phase. The PS_{20k}-*b*-EBR_{60k}-*b*-PE_{6k} copolymer displayed elongated PS cylinders, and consistently is more affected by the continuity of rigid domains, with a yield point at σ_Y = 2.8 MPa, an immediate loss of elastic recovery to 85 % from the first stretching cycle, but also a strong reinforcement with σ_b = 9.2 MPa.
Comparison of these properties with PE_{6k}-*b*-EBR_{60k}-*b*-PE_{6k} previously reported (See Fig. 3a, 3b and S16a) demonstrated that better compromises of properties can be reached with glassy-soft-crystalline than with crystalline-soft-crystalline triblocks. PS_{10k}-*b*-EBR_{60k}-*b*-PE_{6k} shows in particular a strong strain hardening effect leading to high stress at break σ_{max} = 6.2 MPa, while displaying outstanding strain recovery (>95 % after 9 cycles) and a strong shear-thinning at 150 °C leading to comparable viscosities during processing.
All of this information points to a high potential for this copolymer as a TPE material.

Conclusion

The controlled synthesis of various PS-*b*-EBR reference diblock copolymers using a macro-CTA (PS-MgMes) demonstrates the robustness of the switch method from anionic polymerization to CCTP for the design of block copolymers. Asymmetric PS-*b*-EBR-*b*-PE triblock copolymers, incorporating segments of glassy PS, soft EBR and semi-crystalline PE in the same chain, were prepared for the first time with high precision by switching from anionic polymerization to CCTcoP. A variety of materials featuring different mechanical properties depending on the macromolecular architecture of the copolymers obtained (mass fraction of glassy segments). The analysis of the nanoscale morphology of these TPE indicates a phase separation between PS and EBR-PE domains in the melt (> 150 °C), followed by a confined crystallization of PE segments at lower temperatures. This results in a hierarchical self-assembly with EBR rubbery blocks anchored to glassy PS domains on one side, and to PE crystallites on the other side. The most promising copolymer as a TPE material is PS_{10k}-*b*-EBR_{60k}-*b*-PE_{6k} triblock copolymer, presenting a bicontinuous morphology and demonstrating excellent compromises between extensibility (above 1400 %), tensile strength (above 6 MPa), strain recovery (above 95 %) and processability.

Acknowledgements

The authors thank the Centre National de la Recherche Scientifique (CNRS) for funding under the interdisciplinary program ’80 Prime’, and the Manufacture Française des Pneumatiques Michelin for support. They also thank the NMR Polymer Center of Institut de Chimie de Lyon (FR5223) for access to the NMR facilities and assistance. The authors acknowledge the Consortium Lyon Saint-Etienne de Microscopy (CLYM, FED 4092) for the access to the AFM microscope. The AFM characterization was supported by the LABEX iMUST of the University of Lyon (ANR-10-LABX-0064), created within the "Plan France 2030" set up by the french government and managed by the French National Research Agency (ANR). We acknowledge SOLEIL for provision of synchrotron radiation facilities (Swing beamline) and thank Thomas Bisien for assistance.

Keywords: Block copolymers • thermoplastic elastomers • polyolefins • anionic polymerization • Coordinative Chain Transfer Polymerization (CCTP)

References:

[1] G. Zanchin, G. Leone, *Prog. Polym. Sci.* **2021**, *113*, 101342.
[2] H. E. Park, J. M. Dealy, G. R. Marchand, J. Wang, S. Li, R. A. Register, *Macromolecules* **2010**, *43*, 6789–6799.
[3] G. Holden, R. Milkovich, *Block Polymers of Monovinyl Aromatic Hydrocarbons and Conjugated Dienes*, **1966**, US3265765A.
[4] L. Wu, E. W. Cochran, T. P. Lodge, F. S. Bates, *Macromolecules* **2004**, *37*, 3360–3368.
[5] C. De Rosa, R. Di Girolamo, A. Malafronte, M. Scoti, G. Talarico, F. Auriemma, O. Ruiz de Ballesteros, *Polymer* **2020**, *196*, 122423.
[6] S. Bensason, J. Minick, A. Moet, S. Chum, A. Hiltner, E. Baer, *J. Polym. Sci. Part B Polym. Phys.* **1996**, *34*, 1301–1315.
[7] S. Guo, H. Fan, Z. Bu, B. Li, S. Zhu, *Macromol. Chem. Phys.* **2014**, *215*, 1661–1667.
[8] L. Guo, S. Dai, X. Sui, C. Chen, *ACS Catal.* **2016**, *6*, 428–441.
[9] M. Sun, Y. Xiao, K. Liu, X. Yang, P. Liu, S. Jie, J. Hu, S. Shi, Q. Wang, K. H. Lim, Z. Liu, B. Li, W. Wang, *Can. J. Chem. Eng.* **2023**, *101*, 4886–4906.
[10] A. Hotta, E. Cochran, J. Ruokolainen, V. Khanna, G. H. Fredrickson, E. J. Kramer, Y.-W. Shin, F. Shimizu, A. E. Cherian, P. D. Hustad, J. M. Rose, G. W. Coates, *Proc. Natl. Acad. Sci.* **2006**, *103*, 15327–15332.
[11] W. Liu, K. Zhang, H. Fan, W. Wang, B. Li, S. Zhu, *J. Polym. Sci. Part A Polym. Chem.* **2013**, *51*, 405–414.
[12] H. Ohtaki, F. Deplace, G. D. Vo, A. M. LaPointe, F. Shimizu, T. Sugano, E. J. Kramer, G. H. Fredrickson, G. W. Coates,

Macromolecules **2015**, *48*, 7489–7494.
[13] V. C. Gibson, *Science* **2006**, *312*, 703–704.
[14] R. Kempe, *Chem. – A Eur. J.* **2007**, *13*, 2764–2773.
[15] L. R. Sita, *Angew. Chemie Int. Ed.* **2009**, *48*, 2464–2472.
[16] A. Valente, G. Stoclet, F. Bonnet, A. Mortreux, M. Visseaux, P. Zinck, *Angew. Chemie Int. Ed.* **2014**, *53*, 4638–4641.
[17] D. J. Arriola, E. M. Carnahan, P. D. Hustad, R. L. Kuhlman, T. T. Wenzel, *Science* **2006**, *312*, 714–719.
[18] S. D. Kim, T. J. Kim, S. J. Kwon, T. H. Kim, J. W. Baek, H. S. Park, H. J. Lee, B. Y. Lee, *Macromolecules* **2018**, *51*, 4821–4828.
[19] S. S. Park, C. S. Kim, S. D. Kim, S. J. Kwon, H. M. Lee, T. H. Kim, J. Y. Jeon, B. Y. Lee, *Macromolecules* **2017**, *50*, 6606–6616.
[20] D. H. Kim, S. S. Park, S. H. Park, J. Y. Jeon, H. B. Kim, B. Y. Lee, *RSC Adv.* **2017**, *7*, 5948–5956.
[21] V. Monteil, R. Spitz, F. Barbotin, C. Boisson, *Macromol. Chem. Phys.* **2004**, *205*, 737–742.
[22] J. Thuilliez, L. Ricard, F. Nief, F. Boisson, C. Boisson, *Macromolecules* **2009**, *42*, 3774–3779.
[23] I. Belaid, B. Macqueron, M.-N. Poradowski, S. Bouaouli, J. Thuilliez, F. Da Cruz-Boisson, V. Monteil, F. D'Agosto, L. Perrin, C. Boisson, *ACS Catal.* **2019**, *9*, 9298–9309.
[24] M. Langlais, N. Baulu, S. Dronet, C. Dire, F. Jean-Baptiste-dit-Dominique, D. Albertini, F. D'Agosto, D. Montarnal, C. Boisson, *Angew. Chemie Int. Ed.* **2023**, *62*, DOI 10.1002/anie.202310437.
[25] H. Schmalz, V. Abetz, R. Lange, *Compos. Sci. Technol.* **2003**, *63*, 1179–1186.
[26] H. Schmalz, A. Böker, R. Lange, G. Krausch, V. Abetz, *Macromolecules* **2001**, *34*, 8720–8729.
[27] N. Baulu, M. Langlais, R. Ngo, J. Thuilliez, F. Jean-Baptiste-dit-Dominique, F. D'Agosto, C. Boisson, *Angew. Chemie Int. Ed.* **2022**, *61*, DOI 10.1002/anie.202204249.
[28] W. Nzahou Ottou, S. Norsic, M. N. Poradowski, L. Perrin, F. D'Agosto, C. Boisson, *Polym. Chem.* **2018**, *9*, 3262–3271.
[29] J. F. Pelletier, A. Mortreux, X. Olonde, K. Bujadoux, *Angew. Chemie (International Ed. English)* **1996**, *35*, 1854–1856.